Formation Control of Skid-Steered Vehicles Based on Distributed Model Predictive Control

Wang, Yiping; Li, Xueyuan; Liu, Qi; Li, Songhao; Luan, Tian; Li, Zirui

DOI
10.1007/978-981-99-0479-2_113

Publication date
2023

Document Version
Final published version

Published in
Proceedings of 2022 International Conference on Autonomous Unmanned Systems, ICAUS 2022

Citation (APA)
Wang, Y., Li, X., Liu, Q., Li, S., Luan, T., & Li, Z. (2023). Formation Control of Skid-Steered Vehicles Based on Distributed Model Predictive Control. In W. Fu, M. Gu, & Y. Niu (Eds.), *Proceedings of 2022 International Conference on Autonomous Unmanned Systems, ICAUS 2022* (1 ed., Vol. 1010, pp. 1244-1256). (Lecture Notes in Electrical Engineering; Vol. 1010 LNEE). Springer. https://doi.org/10.1007/978-981-99-0479-2_113

Formation Control of Skid-Steered Vehicles Based on Distributed Model Predictive Control

Yiping Wang[1], Xueyuan Li[1(✉)], Qi Liu[1], Songhao Li[1], Tian Luan[1], and Zirui Li[1,2]

[1] The School of Mechanical Engineering, Beijing Institute of Technology, Beijing, China
lixueyuan@bit.edu.cn

[2] Department of Transport and Planning, Faculty of Civil Engineering and Geosciences, Delft University of Technology, Stevinweg 1, 2628 CN Delft, The Netherlands

Abstract. The skid-steered vehicle has the advantages of simple structure and strong maneuverability. Its formation driving can effectively improve safety, reduce energy consumption and exert its benefits, and has wide application prospects in military and civilian fields. Differential skid steering has strong horizontal and vertical coupling characteristics, so the tracking performance of the vehicle is poor. Therefore, it is of great significance to study horizontal and vertical joint control. Firstly, the mathematical model of the vehicle platoon is established to realize the formation control of skid-steered vehicles. Then, a combined horizontal and vertical control strategy for skid-steered vehicle formation is proposed, and a distributed model predictive controller is designed. Finally, simulation experiments verified that the designed method has good feasibility and stability.

Keywords: Skid-steered vehicle · Formation driving · Lateral and longitudinal control · Distributed model predictive control

1 Introduction

A skid-steered vehicle is a vehicle that drives by actively controlling the rotational speeds of the wheels on both sides to form a speed difference [1]. Compared with Ackerman steered vehicles, skid-steered vehicles have a simple structure, high reliability, strong maneuverability, fast operation, and flexible steering and have been gradually applied to wheeled vehicles [2]. At present, multiple countries have studied wheeled skid-steered vehicles, including the RoBattle unmanned vehicle developed by Israel Aerospace Industries (IAI) in 2016 and the J8 Atlas XTR unmanned vehicle developed by Canadian ARGO in 2017, as shown in Fig. 1.

Currently, the focus of wheeled differential steering vehicles is mainly in the field of application and control. The skid-steered vehicle formation technology has broad application prospects in the military, which can effectively reduce the driver's work intensity and improve passability, which has excellent military significance in future wars [3–5]. The main goal of platoon control is to ensure that all vehicles in the platoon move at the same speed while maintaining a pre-set distance from any continuously following vehicle [6].

W. Fu et al. (Eds.): ICAUS 2022, LNEE 1010, pp. 1244–1256, 2023.
https://doi.org/10.1007/978-981-99-0479-2_113

a. the RoBattle unmanned vehicle **b. the J8 Atlas XTR unmanned vehicle**

Fig. 1. Application of wheeled skid-steered vehicles in various countries.

So far, formation control has been studied from different angles and fields. Several typical formation control strategies are proposed, such as leader-follower [7], artificial potential field, and formation control strategy based on virtual structure. Among them, the leader/follower method is the most commonly used in the formation control of unmanned systems. The principle is that the leading vehicle acts as the leader to generate a reference trajectory for the follower vehicle. The follower vehicle as the follower must maintain a certain distance and orientation relative to the leader, ensuring the formation's stability. Zhang W X et al. [8] proposed a three-wheeled mobile robot kinematic model based on the pilot formation control method and a feedback linearization control strategy based on multi-robot steady-state formation control under error-free speed tracking and interference-free conditions. The feedback linearized kinematics model was applied to the dynamic state research when studying the formation control of the differential steering robot [9]. The advantage of the leader/follower method is that it is intuitive and easy to understand; however, this method has the problem of error conduction. Once the leader is disturbed, the entire formation will be affected [10].

Distributed model predictive control has been widely used in formation control due to its small calculation amount, improved system real-time performance, scalability, high reliability, and easy maintenance[11, 12]. When Wei Shanbi et al. [11] studied the distributed model predictive control of the formation control problem of multi-agent systems, they further improved the coherence of agent actions. When the tracking target set point changes, Feramosca et al. [13] presented a cooperative distributed tracking strategy based on linear model predictive control, which can ensure that the system converges to a centralized optimal point. Nascimento [14] presented a predictive controller design scheme based on a nonlinear formation model. Li Keqiang et al. [15] proposed a distributed model predictive control algorithm for vehicle longitudinal formation control, which mainly solves the problem of longitudinal formation control in vehicle formation.

The structure of the paper is as follows: Section 2 introduces the platoon model for the formation problem, including the platoon structure and the vehicle's three-degree-of-freedom dynamics model. Section 3 designs a distributed model predictive controller. Section 4 verifies the feasibility of the proposed controller through simulation experiments and discusses the experimental results. Finally, Section 5 summarizes the work of this paper and makes suggestions for future work.

2 Formation Mathematical Model

2.1 Vehicle Dynamics Model

In the vehicle platoon control problem, the vehicle dynamics model is significant, and the model's accuracy will directly determine the quality of the control effect. The vehicle studied in this paper is a four-wheel skid-steered vehicle. In order to simplify the model, this paper only considers the horizontal plane motion of the vehicle. A three degree-of-freedom dynamic model is established to analyze the dynamic characteristics of four-wheel skid-steered vehicles in longitudinal, lateral, and yaw directions in Fig. 2.

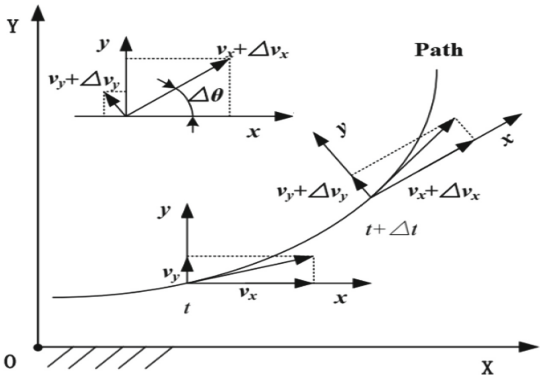

Fig. 2. Schematic diagram of vehicle movement.

The vehicle driving form is that the left and right drive motors drive the left and right wheels through the synchronous belt. The intermediate control variables straight driving torque T_d and steering torque T_s are introduced. The relationship between the two and the torques T_l and T_r output by the left and right motors through the reducer can be expressed as:

$$\begin{aligned} T_d &= T_l + T_r \\ T_s &= T_r - T_l \end{aligned} \tag{1}$$

Through the above analysis, a simplified three-degree-of-freedom dynamic model suitable for this study can be derived as follows:

$$\begin{cases} \dot{v}_x = -f \cdot g + \frac{T_d}{mr} \\ \dot{v}_y = -\frac{4v_y}{mv_x} - \left(\frac{2}{mv_x}(a-b)\cdot k_y + v_x\right)\omega \\ \dot{\omega} = -\frac{2Lk_y}{Iv_x}v_y - \frac{2k_y}{Iv_x}(a^2-b^2)\omega + \frac{BT_s}{2Ir} \end{cases} \tag{2}$$

where f is the rolling resistance coefficient, g is the acceleration of gravity, m is the mass of the vehicle, r is the wheel radius, a is the distance from the center of mass to the front axle, b is the distance from the center of mass to the rear axle, L is the length of the vehicle body, B is the width of the vehicle body, and I is the moment of inertia

around the z-axis, k_x and k_y represent the longitudinal and lateral slip stiffness of the tire, ω represents the yaw rate of the vehicle.

When vehicles are in formation, the vehicle position will become crucial new state information. Therefore, the model is discretized and further expressed in a more general form:

$$\begin{aligned} \xi(t+1) &= \xi(t) + f(\xi(t), u(t))\Delta T \\ q(t+1) &= C\xi(t+1) \end{aligned} \tag{3}$$

where $\xi(t) = [X(t),\ Y(t),\ v_x(t),\ v_y(t),\ \theta(t),\ \theta(t)]^{\mathrm{T}}$, $u(t) = [u_d,\ u_s]^{\mathrm{T}}$, $C = I_6$.

2.2 Spacing Control Strategy

The control goal of vehicle formation is to keep all formation vehicles at the desired distance and speed. The preferred distance and vehicle speed can be achieved through the vehicle distance control strategy, definition $d_{i-1,i}$ is the desired space between the vehicles $i-1$ and i. $d_{i-1,i}$ can be composed of desired distance and desired angle, etc., which determine the geometry of the vehicle queue. The interval strategy used in this study is $d_{i-1,i} = d_0$.

2.3 Communication Topology

In this study, the leader-follower formation method is chosen. The leader is recorded as the serial number 0, located at the leading vehicle position, and the following vehicle number is represented by $1, 2, ...N$, that is, a total of $N+1$ vehicles are in the queue. Vehicles interact according to a specific communication topology. In this paper, a directed graph $G_N = \{v_N, \varepsilon_N\}$ is used to represent the direction of information flow between vehicles. $v_N = \{1, 2, ...N\}$ is the vertex set of vehicle formation; the edge set of the directed graph is defined as ε.

The mathematical model of the communication topology network structure in this study will be given below:

- The adjacency matrix represents the relationship between vehicle nodes, which is defined as: $\boldsymbol{A}_N = \left[a_{ij}\right] \in R^{N\times N}$. Where a_{ij} x represents the weight of the edge of the directed graph, then:

$$a_{ij} = \begin{cases} 1, & \text{if } (i,j) \in \varepsilon_N \\ 0, & \text{if } (i,j) \notin \varepsilon_N \end{cases}, i, j \in N \tag{4}$$

- Define the in-degree of the graph $\mathbf{G}_N = \{v_N, \varepsilon_N\}$ as $deg_i = \sum_{j=1}^{N} a_{ij}$, then the Laplace matrix $\boldsymbol{L}_N$ is $\boldsymbol{L}_N = \boldsymbol{D}_N - \boldsymbol{A}_N$, where $\boldsymbol{D_N} = \begin{bmatrix} deg_1 & & \\ & \ddots & \\ & & deg_N \end{bmatrix}$.

- The traction matrix P represents the information interaction method between the following vehicle and the leading vehicle in the vehicle formation and is defined as:

$$\boldsymbol{P} = \begin{bmatrix} P_1 & & \\ & \ddots & \\ & & P_N \end{bmatrix}$$

where $P_j = \begin{cases} 1, & \text{if } (0,j) \in \varepsilon_{N+1} \\ 0, & \text{if } (0,j) \notin \varepsilon_{N+1} \end{cases}, j \in N.$

3 Controller Design

3.1 Control Objectives

In the horizontal and vertical formation state, to ensure safety, the remaining nodes in the queue all adopt the desired path of the leading vehicle. The distance between vehicles is obtained by integrating the driving route, namely: $S = \int_a^b \sqrt{1 + f'(x)^2} dx$, where $f(x)$ is the path fitting function. Therefore, the control objectives of the vehicle formation are as followers:

$$\begin{cases} f(X) - Y = 0 \\ \theta - arctan\left(f'(X)\right) = 0 \\ \lim\limits_{t\to\infty} \|v_i(t) - v_{i-1}(t)\| = 0 \\ \lim\limits_{t\to\infty} \|S_{i,j} - d_{i,j}\| = 0 \end{cases}, i, j \in N \tag{5}$$

The first term in formula 8 is the lateral tracking error, and the second is the heading error of tracking. These two items describe the vehicle path tracking control target. The third item is the speed of the follower following the preceding vehicle, and the fourth is the speed of the follower and the primary vehicle. The error between the distance of the preceding vehicle and the expected distance, the latter two describe the vehicle formation control objective.

3.2 Node Optimal Subproblem

This section will build a distributed model to predict the multi-objective joint optimization function. The adopted communication topology is the preceding vehicle-following communication topology network structure. That is, the information adopted at every node is the information of the prior vehicle. Define the prediction time-domain predicted by the model as N_p. Define the following three types of variables:

- State variables

  $q_i^p(k|t)$: the predicted pose of the vehicle i in the kth prediction time domain at time t;

  $q_i^*(k|t)$: the optimal pose of vehicle i in the kth prediction time domain at time t;

  $q_i^a(k|t)$: the assumed pose of the vehicle i in the kth prediction time domain at time t;

- Control variables
  $u_i^p(k|t)$: Predictive control amount of vehicle i in the kth prediction time domain at time t;
  $u_i^*(k|t)$: the optimal control amount of vehicle i in the kth prediction time domain at time t;
  $u_i^a(k|t)$: the assumed control amount of vehicle i in the kth prediction time domain at time t;

Therefore, the multi-objective collaborative optimization problem of vehicle nodes in the prediction time domain is obtained as:

$$u_i^*(:|\ t) = argmin\sum\nolimits_k J(k|t) = argmin\sum\nolimits_{k=0}^{N_p-1} P_1\|E_Y(k|t)\|_2 + \sum\nolimits_{k=0}^{N_p-1} P_2\|E_\theta(k|t)\|_2 +$$
$$\sum\nolimits_{k=0}^{N_p-1} P_3\|v_i^*(k|t) - v_{i,dss}(k|t)\|_2 + \sum\nolimits_{k=0}^{N_p-1} P_4\|s_i^*(k|t) - s_i^a(k|t)\|_2 +$$
$$\sum\nolimits_{k=0}^{N_p-1} P_5\|s_i^*(k|t) - s_{i-1}^a(k|t) - d_{i,i-1}\|_2 + \sum\nolimits_{k=0}^{Np-1} P_6\|u_d^*(k|t) -$$
$$u_d^*(k+1|t)\|_2 + \sum\nolimits_{k=0}^{N_p-1} P_7\|u_s^*(k|t) - u_s^*(k+1|t)\|_2 \tag{6}$$

subject to

$$\begin{aligned}
&\xi_i^*(k+1|t) = \xi_i^*(k|t) + f(\xi^*(k|t), u_i^*(k|t))\Delta T\\
&q_i^*(k|t) = C\xi_i^*(k|t)\\
&s_i^*(k|t) = q_i^*(k|t)_{(1:2)}\\
&E_Y(k|t) = f(x_i^*(k|t)) - y_i^*(k|t)\\
&E_\theta(k|t) = \theta_i^*(k|t) - arctan(f'(x_i^*(k|t)))\\
&s_i^*(N_P|t) = s_{(i-1)}^a(N_P|t) - d_{(i,i-1)}\\
&u_i^*(N_P|t) = u_{(i,\,des)(N_P|t)}\\
&u_{min}in \le u_i^*(k|t) \le u_{max}
\end{aligned}$$

In the optimization function, $P_1, P_2, P_3, P_4, P_5, P_6, P_7$ is the weight coefficient of each optimization objective. For the vehicle node, E_Y and E_θ represent the tracking error and heading error of the desired path, and $v_{i,des}$ represents the expected speed of the vehicle. This item represents the error of the vehicle tracking queue's expected speed. The fourth term describes the error between the optimal trajectory of the vehicle node t at time $t+1$ and the assumed circuit at time t, and the establishment of this error term penalizes the degree to which the vehicle deviates from the assumed trajectory. The fifth item represents the error between the distance between the optimal predicted course of node i at time $t+1$, and the assumed trajectory of node $i-1$ in its domain at time t for time $t+1$ and the expected distance. The last two items represent the weight of the variation of the vehicle control amount. This weight makes the speed change of the vehicle as small as possible so that the vehicle control process becomes smooth.

3.3 Control Algorithm Flow

This study assumes that the communication delay in the vehicle formation is not considered, and the optimization problem can be solved within one prediction step. The flow of the control algorithm is shown in Fig. 3.

1. Initialization, at time $t = 0$, assuming that all vehicles in the queue move in a straight line at a uniform speed, the state, and control amount of the vehicles at this time are:

$$\begin{aligned} \xi_i^a(k+1|0) &= \xi_i^p(k+1|0) \\ u_i^a(k+1|0) &= u_i(0) \end{aligned} \tag{7}$$

   where $k = 1, 2, ...N_P - 1$.
2. At any time t, for each vehicle node, cycle through the following steps:

   a. Using the current state q_i, assuming the output state $q_i^a(k|t)$, the assumed output state $q_{-i}^a(k|t)$ of the preceding vehicle and the expected state $q_{i,des}(k|t)$ of the leading vehicle (if available), solve the current sub-optimization problem J_i to obtain the optimal control sequence $u_i^*(k|t)$.
   b. Apply the control variable $u_i^*(0|t)$ to the vehicle node to obtain the vehicle state q_i at the next moment.
   c. Use the optimal control sequence $u_i^*(k|t)$ to calculate the optimal state $q_i^*(k+1|t)$ of the vehicle node in the predicted time domain.
   d. Calculate the hypothetical state $q_i^a(k+1|t+1)$ of the vehicle node in the predicted time domain using the hypothetical control sequence $u_i^a(k|t+1)$, where

$$u_i^a(k|t+1) = \begin{cases} u_i^*(k+1|t), & k = 0, 1, \cdots, N_p - 2 \\ u_i(0), & k = N_P - 1 \end{cases}.$$

   e. Send $q_i^a(k|t+1)$ to the following car, and receive $q_{-i}^a(k|t+1)$ sent by the preceding car. If the code connects to the pilot car, receive $q_{i,des}(k|t+1)$.

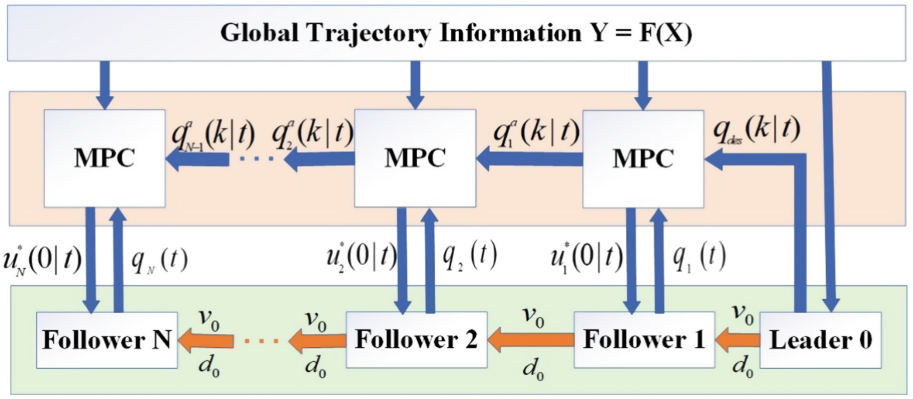

Fig. 3. Control algorithm flow.

4 Simulation and Result Analysis

4.1 Simulation Scene Construction

This study is mainly based on the research center's skid-steered vehicle queue, so a homogeneous row of four vehicles is considered, including one leading vehicle and

three following vehicles. The real parameters of each vehicle in the research center are shown in Table 1, and the topological structure of vehicle-to-vehicle communication is the preceding vehicle-following type. In this paper, the primary purpose of the horizontal and vertical control of vehicle formation is to realize the lane-changing condition of vehicle formation. Therefore, the leading vehicle adopts a double-lane change trajectory and has a significant acceleration before changing lanes. The vehicle's initial speed is set to 8 m/s, the rate reaches 10 m/s after 1s of linear acceleration, and the vehicle enters the lane-changing condition. Select the prediction step size $\Delta t = 0.1s$, the prediction time domain $N_P = 20$, and set the input limit as $-200 < u_i < 200$ according to the actual situation of the vehicle.

Table 1. Main parameters of the vehicle

Vehicle parameters	Symbol	Value
Vehicle Quality	m	200 kg
Wheel Radius	r	0.25 m
Distance from Center of Mass to Front axle	a	0.55 m
Distance from Center of Mass to Rear axle	b	0.45 m
Vehicle length	L	1.0 m
Vehicle width	B	0.5 m
The Moment of Inertia of the Vehicle about the Z-axis	I	36 kg·m^2
Tire Cornering Stiffness	k_y	66900
Rolling Resistance Coefficient	f	0.01

In the simulation, the expected distance between vehicles is set to $d_{i-1,i} = 10m$, and the initial error of the distance between vehicles is 0. To study the influence of different weight coefficients on the platoon formation effect and path tracking accuracy, this paper selects eight groups of varying weight coefficients. The weight coefficients set in other group are different from those set in group B, as shown in Table 2.

Table 2. Optimization problem weight coefficients

Group	P1	P2	P3	P4	P5	P6	P7
B	1	1	1	1	1	1	1
A1	10	1	1	1	1	1	1
A2	1	10	1	1	1	1	1
A3	1	1	10	1	1	1	1
A4	1	1	1	10	1	1	1
A5	1	1	1	1	10	1	1
C1	1	1	1	1	1	10	1
C2	1	1	1	1	1	1	10

4.2 Result Analysis

In this data simulation, the mean and standard deviation of the tracking, speed, and formation errors for eight groups of different weight coefficients can be obtained according to the simulation test results, which are recorded in Table 3. The analysis of Table 3 shows that the errors of the A2 group in the multiple groups of weight coefficients are all small, indicating that the weight P2 of the heading error significantly affects the control effect of the vehicle formation. The influence of P2 on the formation error is the most obvious, and the increase of P2 is beneficial in reducing the formation error.

Table 3. Error situation under different weight coefficients

Group	Tracking error		Speed error		Formation error	
	average value	standard deviation	average value	standard deviation	average value	standard deviation
B	0.1295	0.2128	0.3944	0.6307	0.1967	0.3077
A1	0.1235	0.1999	**0.2987**	**0.4385**	0.1733	0.2496
A2	**0.1250**	**0.2033**	**0.3068**	**0.4525**	**0.1615**	**0.2402**
A3	0.1279	0.2059	0.3349	0.5129	0.1710	0.2411
A4	0.1243	0.2010	0.3158	0.4830	0.1702	0.2322
A5	**0.1207**	**0.2000**	0.3331	0.4917	0.1793	0.2585
C1	0.1221	0.2019	0.3020	0.5314	0.1661	0.2667
C2	0.1282	0.2081	0.3429	0.4801	0.1801	0.2513

In addition, it can be seen from the data in Table 3 that the main influencing factor of vehicle tracking error is P5, and the main influencing factor of vehicle speed error is P1. The analysis shows that the larger weight coefficient P5 and the larger weight coefficient P1 are more conducive to reducing the error.

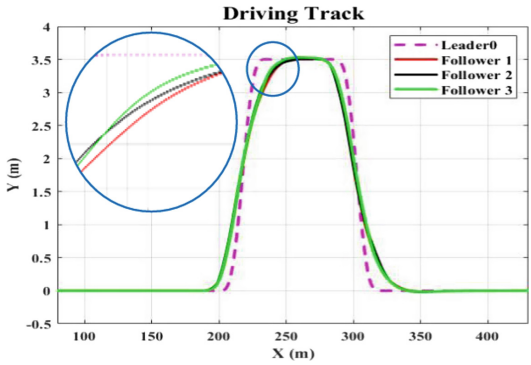

Fig. 4. Vehicle formation driving trajectory.

According to the above analysis, the simulation results of group A2 are selected to analyze the controller's performance. In this data simulation, the leading vehicle is driving a lane-changing trajectory, as shown in the driving rotation 0 in Fig. 4. Figure 4 is a vehicle formation moving trajectory diagram. Figure 5 shows the lateral positions of the vehicle nodes. Figure 6 is a diagram of the vehicle formation offset trajectory error. From Fig. 5 and Fig. 6, it can be seen that the tracking error is maintained within 0.05 m until 13 s. At the 13 s, the formation begins to enter the lane-changing condition, and the lateral tracking error of the vehicle to the desired trajectory gradually increases. The 2-th generates the maximum error following vehicle, which is 0.67 m. It can be seen that when vehicles are driving in formation, they have high tracking accuracy for the desired trajectory, which can meet the safety and feasibility in lane-changing conditions.

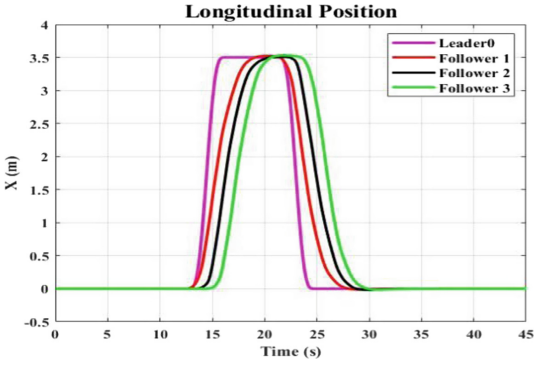

Fig. 5. Vehicle node lateral position.

The main task of vehicle formation control studied in this paper is to keep the vehicle platoon running at a certain speed and keep the exact distance between vehicles. The vehicle formation speed error in the simulation test is shown in Fig. 7, and the formation error curve of the vehicle formation in the simulation test is shown in Fig. 8. It can be seen from the figure that when the leading vehicle enters the linear acceleration condition, the

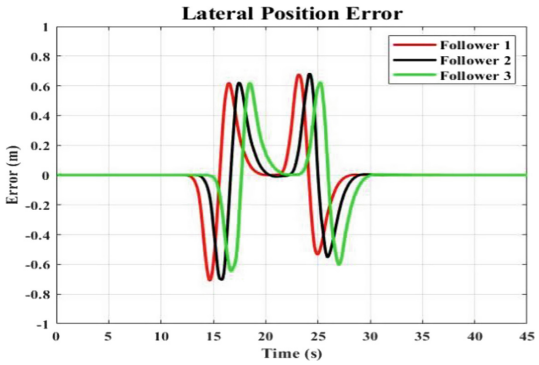

Fig. 6. Vehicle node tracking expected trajectory error.

workshop speed error and formation error begin to change. Still, the maximum values are 0.78 m/s and 0.86 m, respectively, and the control accuracy is high. At 13 s, the formation vehicles begin to enter the lane-changing condition, and the vehicle speed and formation errors start to change. During the street changing process, the speed error fluctuates to a certain extent, and the maximum value reaches 2.47 m/s. The overall control accuracy is high and within the acceptable range of the error. The variation range of the platoon error is all within 1.14 m, and the control effect is good compared to the expected vehicle spacing of 10 m. Through the overall analysis of the speed error and the formation error, in the lane-changing condition, the speed error and the formation error are both small, which can be consistent with the expected formation and expected speed.

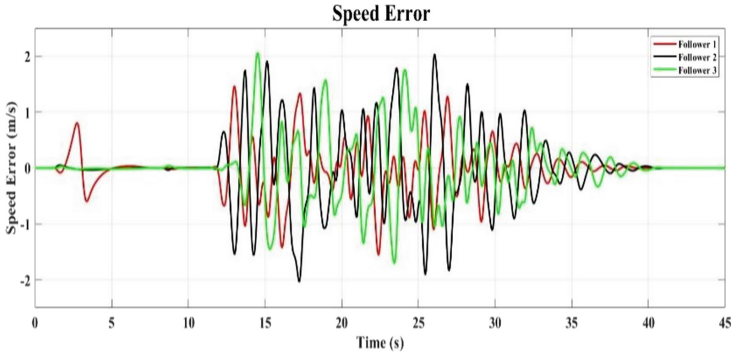

Fig. 7. Vehicle formation speed error.

The simulation results show that the control algorithm based on distributed model prediction established in this paper has a good control effect on the vehicle linear acceleration condition and lane changing situation, and the control accuracy is within the acceptable range, which shows the feasibility of the algorithm.

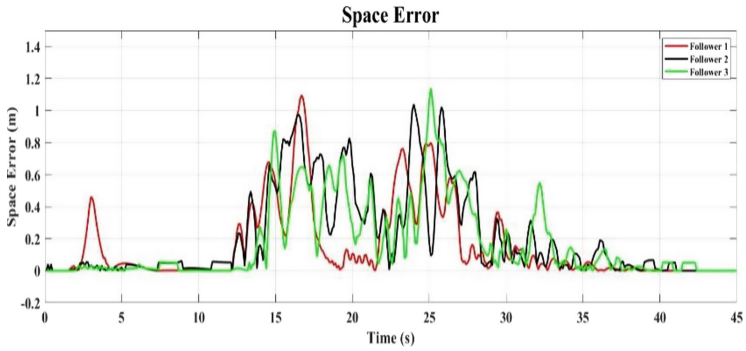

Fig. 8. Vehicle formation error.

5 Conclusions

The main research content of this paper is the formation control problem of skid-steered vehicles. Aiming at this problem, this paper firstly analyzes the mathematical model of the queue, including the dynamic model, communication topology, and queue geometry. Secondly, it is concluded that the vehicle formation system in this study needs to be optimized in coordination. Based on this, a vehicle formation controller based on distributed model prediction is designed in this paper, and data simulation experiments verify the algorithm's feasibility.

In this paper, the control method of the skid-steered vehicle adopts the horizontal and vertical control methods. It has a specific reference value for future intelligent vehicle formation control research. One of the future research directions is to improve the control algorithm, find the influence rule of the weight coefficient of the optimization problem, and increase the stability and robustness of the control algorithm.

References

1. Matraji, I., AlDurra, A., Haryono, A., AlWahedi, K., AbouKhousa, M.: Trajectory tracking control of skid-steered mobile robot based on adaptive second order sliding mode control. Control Eng. Pract. **72**, 167–176 (2018). https://doi.org/10.1016/j.conengprac.2017.11.009
2. Dogru, S., Marques, L.: A physics-based power model for skid-steered wheeled mobile robots. IEEE Trans. Robot. **34**(2), 421–433 (2018). https://doi.org/10.1109/TRO.2017.2778278
3. Li, L., Ji, X., Qu, X., Ran, B.: A macroscopic model of heterogeneous traffic flow based on the safety potential field theory. IEEE Access **9**, 7460–7470 (2021). https://doi.org/10.1109/ACCESS.2021.3049393
4. Hu, Y., Chen, C., He, J., Yang, B.: Eco-platooning for cooperative automated vehicles under mixed traffic flow. IEEE Trans. Intell. Transp. Syst. **22**(4), 2023–2034 (2021)
5. Xie, D.-F., Zhao, X.-M., He, Z.: Heterogeneous traffic mixing regular and connected vehicles: modeling and stabilization. IEEE Trans. Intell. Transp. Syst. **20**(6), 2060–2071 (2018)
6. Hu, B., Lemmon, M.D.: Distributed switching control to achieve almost sure safety for leader-follower vehicular networked systems. IEEE Trans. Autom. Control **60**(12), 3195–3209 (2015)

7. Shladover, S.E., et al.: Automated vehicle control developments in the PATH program. IEEE Trans. Veh. Technol. **40**(1), 114–130 (1991)
8. Zhang, W.X., Yuan, J.: Formation control based on backstepping trajectory tracking control for multiple mobile robots. Autom. Instrum. (2016)
9. Dierks, T., Jagannathan, S.: Neural network output feedback control of robot formations. IEEE Trans. Syst. Man Cybern. Part B (Cybern.) **40**(2), 383–399 (2009)
10. Jung, H., Kim, D.H.: Implementation of symmetrical rank based formation for multiple robots. Int. J. Control Autom. Syst. **14**(1), 350–355 (2016). https://doi.org/10.1007/s12555-014-0322-y
11. Wei, S., et al.: Distributed model predictive control for multi-agent systems with improved consistency. J. Control Theory Appl. **8**, 117–122 (2010)
12. Morgan, D., Chung, S.J., Hadaegh, F.Y.: Model predictive control of swarms of spacecraft using sequential convex programming. J. Guid. Control. Dyn. **37**(6), 1725–1740 (2014)
13. Ferramosca, A., Limon, D., Alvarado, I., Camacho, E.F.: Cooperative distributed MPC for tracking. Automatica **49**(4), 906–914 (2013)
14. Nascimento, T.P., Moreira, A.P., Conceição, A.: Multi-robot nonlinear model predictive formation control: moving target and target absence. Robot. Auton. Syst. **61**(12), 1502–1515 (2013)
15. Zheng, Y., Li, S.E., Li, K., Borrelli, F., Hedrick, J.K.: Distributed model predictive control for heterogeneous vehicle platoons under unidirectional topologies. IEEE Trans. Control Syst. Technol. **25**(3), 899–910 (2017)